Growth kinetics of intermetallic compounds and tensile properties of Sn–Ag–Cu/Ag single crystal joint

Hefei Zou, Qingsheng Zhu, Zhefeng Zhang *

*Shenyang National Laboratory for Materials Science, Institute of Metal Research, The Chinese Academy of Sciences,
72 Wenhua Road, Shenyang 110016, PR China*

Abstract

The growth kinetics and interfacial morphologies of intermetallic compounds (IMCs) and tensile properties of single crystal Ag/Sn–3.8Ag–0.7Cu (SAC) solder joint were investigated by solid-state aging at 170 °C and liquid-state aging at 250 °C. It is found that the growth kinetics of IMCs under both solid- and liquid-state aging conditions follow parabola relationship. Accordingly, the diffusion coefficients under the two conditions were calculated to be about 2.50×10^{-17} m^2 s^{-1} and 1.60×10^{-14} m^2 s^{-1}, respectively. With increasing aging time, the scallop-like morphology of the IMC gradually evolved into planar type after solid-state aging; but it became rougher after liquid-state aging. Meanwhile, the average grain size of IMC also increases with increasing aging time. The tensile strength of the Sn–Ag–Cu/Ag single crystal joints did not decrease seriously with increasing aging time and the corresponding tensile fracture mechanism was discussed.
© 2007 Elsevier B.V. All rights reserved.

Keywords: Ag single crystal substrate; Sn–3.8Ag–0.7Cu solder; Intermetallic compounds (IMCs); Growth kinetics; Tensile strength; Fracture

1. Introduction

A series of Sn–Pb solders have been widely used in electronic packaging field because of their excellent electronic conductivity, good wettability, low cost, low melting point, good mechanical properties and good thermal conductivity [1,2]. There are many investigations on the Sn–Pb solders, including growth kinetics of intermetallic compounds (IMCs), wettability, mechanical properties and so on [3–8]. However, due to the environmental concerns arising from the toxicity of Pb, in recent years, Sn–Pb solders had been prohibited in electronic packaging field in USA, Europe and Japan. Therefore, more and more researchers and electronic packaging manufacturers gradually pay much attention to lead-free solders. Nowadays many lead-free solders with copper and nickel substrates have been intensively investigated, including Sn–Ag, Sn–Bi, Sn–Cu, Sn–In and Sn–Zn alloys [1,9–20]. The corresponding investigations involve many fields, including wettability and its mechanism, tensile and shear strengths, isothermal aging on solid-state and

liquid-state and so on. Some reports indicate that shear and tensile strengths intensely drop with increasing aging time and shear strength often increases at higher shear rate [21]. During aging, IMCs are always formed between the solder and the substrate, and often play an important role in the properties of various lead-free solder joints. Normally, it will cause a negative effect on the interfacial strength when an IMC grows thicker under high work temperature condition. In order to retard the interfacial reaction and the growth of IMCs or improve the mechanical properties of the solder joints, electro-plating nickel film on the copper substrate or changing the compositions of the solders (e.g. adding ZrO$_2$, Ni, In into the solder) has been used in the electronic packaging field industry [2,9,10,12,19,22].

On the other hand, it is well known that silver is a good substrate due to its good wettability, anti-oxidation, good electronic and thermal conductivity [23,24]. Silver films have been widely used in the electronic packaging thick-film hybrid integrated circuits (HIC), resistors, ceramic capacitors, multi-layer chip inductors [23]. For example, in the flip chip process, silver film is commonly employed as one of the wetting layers. Among the lead-free solders, Sn–Ag–Cu solder alloy is one of the most promising lead-free solders for its relatively low melting point, low cost, good solderability and excellent mechanical

* Corresponding author. Tel.: +86 24 23971043; fax: +86 24 23891320.
E-mail address: zhfzhang@imr.ac.cn (Z. Zhang).

properties [1,25–27]. But there are few reports on the mechanical properties of the joints between lead-free solders with silver substrate [3,20,23,24,28], especially for the joint between Sn–3.8Ag–0.7Cu (SAC) solder and silver substrate. It is significantly important to carry out some researches on the joint properties between silver substrate and SAC solder. The main objective of the current study is concerned with the morphology and growth kinetics of IMCs formed in Ag/SAC solder joint after solid- and liquid-state aging. In particular, in order to get the fundamental data and avoid the possible effects of grain boundary and crystallographic orientation, Ag single crystal was employed as substrate to reveal the growth kinetics and morphology of the interfacial IMCs after solid- and liquid-state aging. Finally, the tensile strength and fracture mode of the Sn–Ag–Cu/Ag single crystal joints after solid–liquid aging were investigated.

2. Experimental procedure

In this study, silver single crystal (4N) was employed as substrate for electronic packaging with Sn–Ag–Cu solder. The silver single crystal plate with a dimension of 40 mm × 80 mm × 10 mm was grown by the Bridgman method in a horizontal furnace. A lead-free solder alloy with the composition of Sn–3.8Ag–0.7Cu (wt.%) was prepared by melting high purity (4N) tin, silver and copper in vacuum ($>10^{-1}$ Pa) at 800 °C for 30 min. Firstly, a group of Ag sticks with the size of 3 mm × 4 mm × 30 mm was spark-cut from the bulk silver single crystal plate. Secondly, the surface of the Ag single crystal substrate used to solder was ground with 2000#SiC paper; then was carefully polished with 2.5 μm, 1.5 μm, 0.5 μm polish paste, followed by washing in water and ethanol. Thirdly, the polished surface was covered with some rosin flux and a thin piece of solder, as illustrated in Fig. 1. Then the samples were soldered in an oven at a constant temperature of 240 ± 2 °C for several minutes to evaporate the rosin flux, followed by cooling in air condition. For the samples used to observe the morphology and grain size of IMCs, the plate dimension is about 2 mm × 4 mm × 1 mm. After observing the cross-section of the as-reflowed samples, they were put into an oven at a constant temperature of 170 ± 2 °C for isothermal aging 1, 4, 9, 13 and 16 days, respectively. Then the growth kinetics and morphologies of IMCs of the Sn–Ag–Cu/Ag interfaces after different aging time were observed with a LEO super35 or a Cambridge S360 scanning
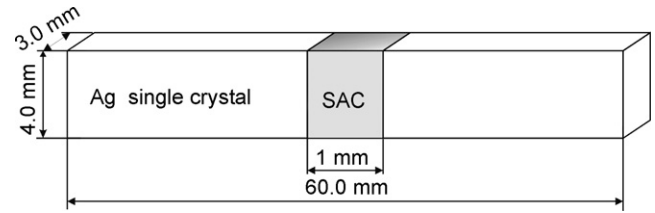

Fig. 1. Schematic diagram of as-prepared SAC/Ag single crystal couple.

electron microscopy (SEM). All the tensile experiments were carried out on an INSTON 8807 testing machine under a constant strain rate of about 5×10^{-4} at room temperature in air. After fracture, the deformation morphologies and fractographies were observed with the SEM.

In order to observe the grain morphology of the IMCs aging for different days, the soldered samples were immersed in a 10 wt% HNO_3 + CH_3OH solution for several hours to dissolve away the excess Sn–Ag–Cu solder and expose the IMCs layer. Then the samples were washed in water and ethanol for a better observation on the IMCs morphology with the high-resolution LEO super35 SEM.

3. Results and discussion

3.1. Morphology and growth kinetics of IMCs under isothermal solid-state aging

Fig. 2 shows the interfacial morphologies of IMCs in the Ag/SAC joints aged at 170 °C for different days. Some scalloplike IMC layers were observed between the (SAC) solder and silver single crystal substrate, as shown in Fig. 2(a)–(e). The diagram of EDX indicates that the IMC is Ag_3Sn phase; however, Ag_5Sn phase was not observed in all the as-reflowed samples. With further aging at 170 °C for different days, there is only Ag_3Sn phase, and Ag_5Sn phase was still not found in all the aged samples, which is well consistent with the most previous observations [20,23,24], albeit there is an exception in the literature [28]. There might be two reasons for that: firstly, the
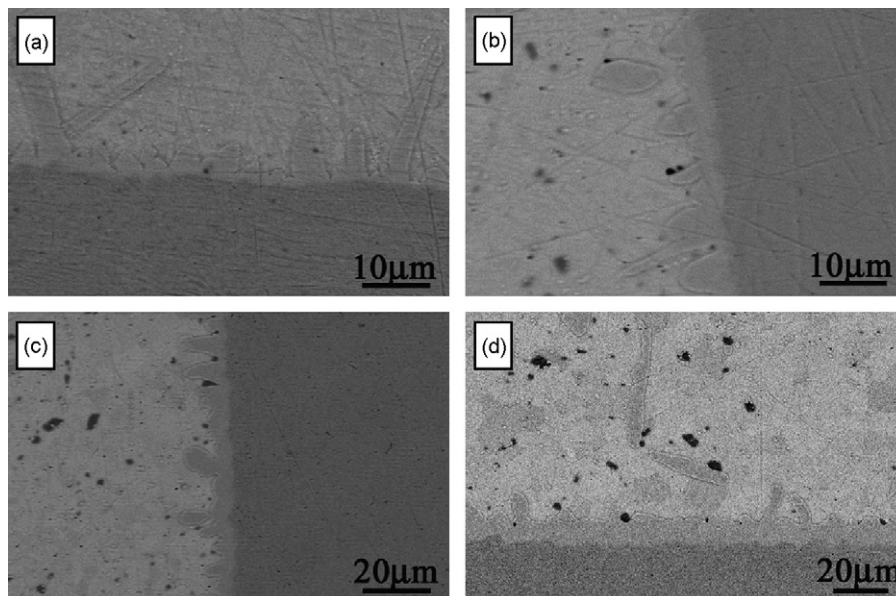

Fig. 2. The morphologies of the IMCs at the SAC/Ag interface on solid-state aging: (a) as-reflowed, aged at 170 °C for (b) 1 day, (c) 4 days and (d) 13 days.

Ag_5Sn layer may be too thin to be detected; secondly, the standard Gibbs function of molar reaction of Ag_5Sn phase is much higher than that of Ag_3Sn phase. From the binary Ag–Sn phase diagram, it is apparent that the melting point of Ag_5Sn phase is higher than that of Ag_3Sn phase. Normally, the material with higher melting point will have higher standard Gibbs function of molar reaction. Besides, the scallop-like IMCs were found to gradually change into planar ones with increasing aging time, which is in accord with that observed in the case of Cu substrates [29,30].

During the solid-state aging, the distance between the solder and silver substrate is different. The distance of the valley of the scallop is closer to the solder than that of the peak region of the scallop. Since the total (bulk) diffusion coefficients of Ag and Sn through Ag_3Sn are nearly the same, the required time of Ag atoms reaching the solder or Sn atoms reaching the Ag substrate should be shorter for the valley region of the scallop. This indicates that the growth velocity in the valley region of the scallop-like IMCs is higher than that in the peak region. As a result, the whole interfacial layer of the IMCs will trend to become planar with increasing aging time. Therefore, the thickness of the IMCs becomes thicker and thicker, leading to a gradually decreasing growth velocity of the IMCs. This is because the time used to diffuse the atoms through the thicker IMC layers is gradually increasing with the increase in thickness of IMCs. As is well known, there is a parabola function between the aging time and the thickness of the IMCs based on abundant data available under the solid-state aging [20,23,29–31]. There are many researches on Sn–Ag–Cu/Cu substrate [29,30,32,33], however, there are few reports on Sn–Ag–Cu/Ag joint, especially on Sn–Ag–Cu/Ag single crystal joint. The morphologies of the IMC layers for all the aged Sn–Ag–Cu/Ag joint samples were observed (see Fig. 2) and the thickness was measured carefully. In this study, in order to decrease the error, both the integral area and the length of the IMC layers were measured
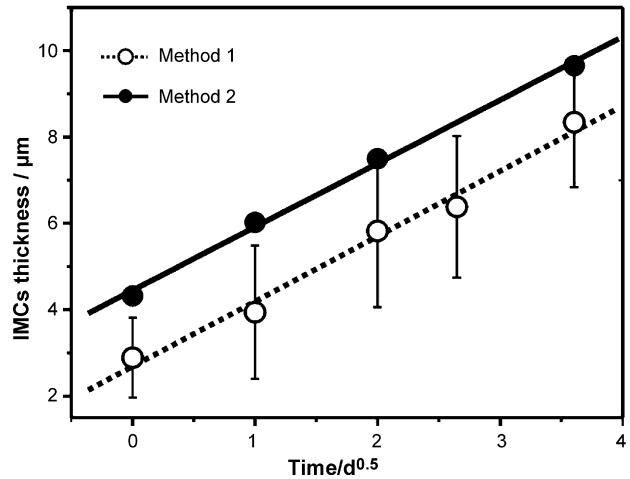

Fig. 3. Plot of the thickness of the Ag_3Sn layer as a function of aging time after solid-state aging at 170 °C. Method 1: the average of thicknesses of many different places. Method 2: the value of the integral area to the width of the IMCs.

using a special software. For example, the average thickness of the IMCs can be calculated by using the following equation:

$$T = \int_0^{L_0} \frac{f(x)\,dx}{L_0}. \tag{1}$$

Here L_0 is the length of the measured region, $f(x)$ is the contour function of the IMCs and T is the average thickness of the IMC layer. It is found that the thickness T of Ag_3Sn IMC layer follows a square root function with the aging time, as solid dots (line) plotted in Fig. 3. Therefore, the diffusion coefficient can be calculated according to the following empirical equation [29,34]:

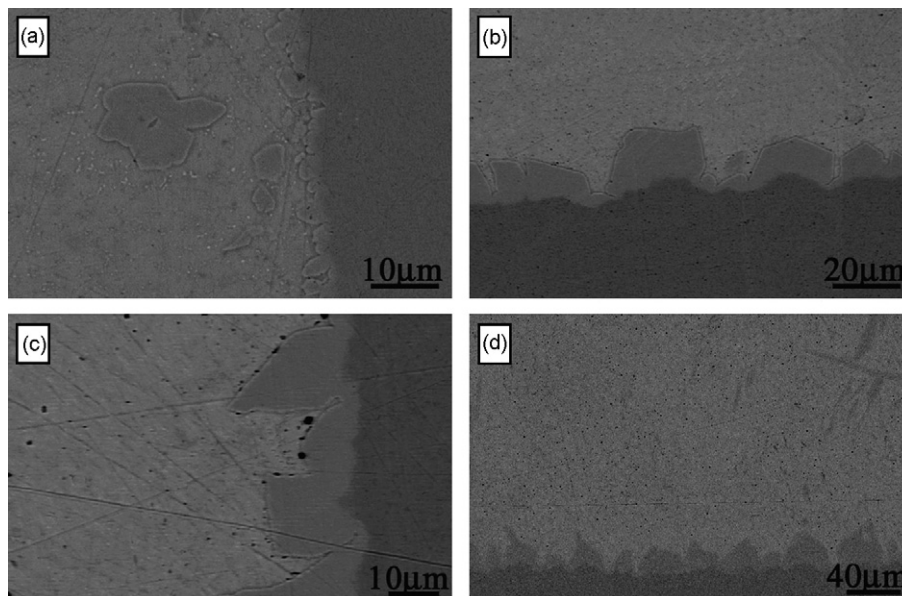$$T = D^{1/2}\sqrt{t} + c, \tag{2}$$

Fig. 4. The morphologies of the IMCs at SAC solder/Ag interface after liquid-state aging: (a) as-reflowed, aging at 250 °C for (b) 30 min, (c) 90 min and (d) 150 min.

where T, t, D, c are the average thickness of the Ag$_3$Sn layer, the aging time, the diffusion coefficient and a constant, respectively. Based on the data (solid dots) in Fig. 3, the value of diffusion coefficient D was calculated as 2.50×10^{-17} m^2 s^{-1} for the Ag$_3$Sn layer. For comparison, the average thicknesses of the IMC layer measured by SEM are also shown in Fig. 3 (see the data with error bar). In this case, the calculated diffusion coefficient is about 2.50×10^{-17} m^2 s^{-1}, which is quite close to the data measured by method one. Also, the current results are smaller than the previous results of Sn–Ag–Cu/Cu joint, for example, 7.24×10^{-17} m^2 s^{-1} aging at 170 °C [29], and slightly higher than the previous results of Sn–Ag–Cu/Ni joint, for example, 1.2×10^{-17} m^2 s^{-1} aging at 175 °C [33]. It implies that Ag might be a good substrate to decrease the growth speed of IMCs during the isothermal solid-state aging except its good wetting behavior. It should be pointed out that actually the value of diffusion coefficient D is the inter-diffusion coefficient, including Ag and Sn atoms diffuse through the Ag$_3$Sn phase because some researchers suggest that D is only the diffusion coefficient of substrate atoms in the bulk substrate or bulk solder [23].

3.2. Microstructure evolution of the IMCs under isothermal liquid-state aging

Fig. 4 shows the morphology of the IMCs formed in the Ag/Sn–Ag–Cu solder joints aging at 250 °C for different hours. The morphologies and the growth kinetics of the IMC layer were also analyzed. With the help of EDX, the IMC is found to be still Ag$_3$Sn phase, which is the same as the IMC after solid-state aging, also indicating that there is no new IMC phase formation even at higher aging temperature. The morphologies of the Ag$_3$Sn layer did not change into the planar one with increasing aging time. It can be seen that the thickness of the Ag$_3$Sn IMCs also obeys the square root function with reacting time, as plotted in Fig. 5, which is similar to the diffusion behavior under the solid-state aging. But there are still some differences
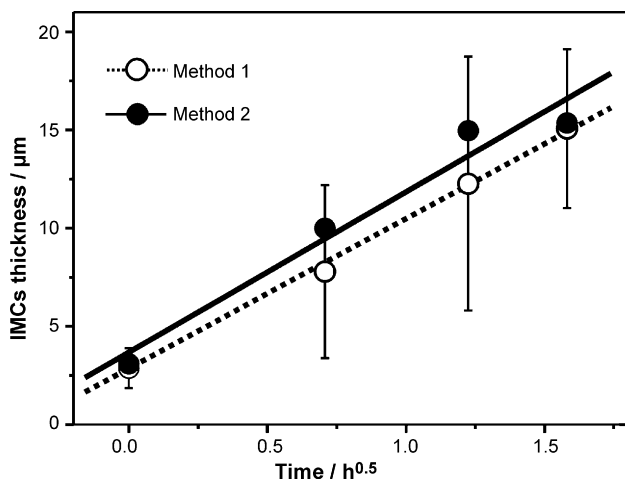

Fig. 5. Plot of the thickness of Ag$_3$Sn layer as a function of aging time after liquid-state aging at 250 °C. Method one: the average of thicknesses of many different places. Method two: the value of the integral area to the width of the IMCs.
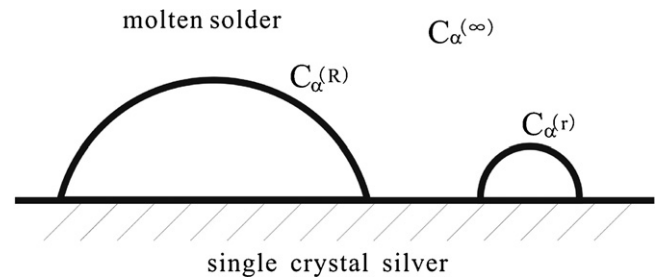

Fig. 6. Schematic diagram illustrate concentration of different grain size of IMCs.

in the growth speed and the morphology of the IMCs between the solid-state and liquid-state aging. Firstly, the growth speed of the Ag$_3$Sn IMCs during the isothermal liquid-state aging is much faster than that during the solid-state aging. Using the empirical equation (1), the value D of the isothermal liquid-state aging was calculated to be about 1.83×10^{-14} m^2 s^{-1} (1.60×10^{-14} m^2 s^{-1} for method one), which is three orders of magnitude higher than that during solid-state aging. This can be explained by the Arrhenius equation, i.e. the higher is the temperature, the more are the active atoms. On the other hand, during the liquid-state aging some Ag atoms in solder or from Ag substrate only require to diffuse through the liquid solder, while Ag atoms have to diffuse through the solid Ag$_3$Sn phase for the solid-state aging. During the isothermal liquid-state aging, the fluxes of Ag atoms consist of two fluxes, i.e. the flux of the interfacial reaction and the flux of ripening [35]. But the resource of the flux of Ag atoms on the isothermal solid-state is only the interfacial flux. Therefore, the liquid-state aging has higher diffusion coefficient D than the solid-state aging.

Compared with the morphology of the IMCs on the solid-state aging, as shown in Fig. 2, it seems that the scallop-like morphology of the IMCs cannot change into planar morphology with increasing aging time. In contrast, the morphology of IMCs often becomes rougher, which may be explained by the Ostwald ripening theory, as illustrated in Fig. 6. The concentration of Ag atoms in the molten Sn–Ag–Cu solder on the surface of the IMC grains follows the Gibbs–Thomson equation [35]:

$$C_\alpha(r) = C_\alpha(\infty) \exp\left(\frac{2\sigma V_{\mathrm{m}}}{rRT}\right) \tag{3}$$

and

$$C_\alpha(r) = C_\alpha(\infty)\left(1 + \frac{2\sigma V_{\mathrm{m}}}{RTr}\right), \quad \text{if } \frac{2\sigma V_{\mathrm{m}}}{RTr} \ll 1, \tag{4}$$

where $C_\alpha(r)$ is the concentration of Ag atoms on the surface of the IMC grains, $C_\alpha(\infty)$ is the equilibrium concentration of Ag atoms in the Sn–Ag–Cu solder, σ is the interfacial energy per unit area between Ag$_3$Sn and molten Sn–Ag–Cu solder, r is the radius of the IMC grains, V_{m} is the molar volume of Ag$_3$Sn, R is a gas constant, and equal to 8.314 J mol^{-1} k^{-1}, and T is the absolute temperature. From this equation, the value of $C_\alpha(r)$ would fall with increasing the value of 'r'. Since the concentration of the Ag atoms in the larger grain surface should be lower than that in the smaller grain, as a result, there is a higher concentration gradient between the larger grain and the melting solder. In other

words, the flux of Ag atoms of the larger grain is higher than that of the smaller grain, which further leads to rougher morphology of the IMCs. With increasing aging time, the large grains grow much larger while the smaller grains are gradually swallowed. In conclusion, the scallop-like IMCs cannot change into planar IMCs during the aging process. But for the solid-state aging, it is not discussed in the same method because the Ag atoms coming from the Ag substrate play a more important role than that of the IMC of interface. Therefore, Ag atoms coming from the IMC interface was ignored.

3.3. Tensile properties of SAC/Ag after solid-state aging

Fig. 7(a) shows one typical tensile stress–strain curve of Sn–Ag–Cu/Ag joint samples aged at 170 °C for 1 day. The tensile stress–strain curve demonsrates that the yielding, deformation and fracture behavior of the solder joint sample is similar to homogenous metallic materials. There are several stages in the stress–strain curve, i.e. elastic deformation, plastic flow with obvious strain-hardening and final fracture. For the other samples aging for different days, they also displayed the similar deformation, plastic flow and fracture feature. Fig. 7(b) shows the dependence of tensile strength of the Sn–Ag–Cu/Ag joint on the aging time. It can be seen that with increasing aging time, the tensile strength gradually decreases, but the decrease degree is very small. However, when the substrate is copper, the tensile strength of the Sn–Ag–Cu/Cu joint decreases dramatically [36]. The reason may be that the residual stress at the Sn–Ag–Cu/Cu joint interface is higher than that of the Sn–Ag–Cu/Ag joint interface. For the copper substrate, Lee et al. [37] observed some cracks existing in the IMCs and the interface when the aged samples were stored for several days at room temperature. But for the Ag substrate joint samples, there is no crack in those regions under the same disposal in this study. Then Lee et al. [37] have calculated the residual stress of the aged samples and found that the residual stress is high enough to pro-
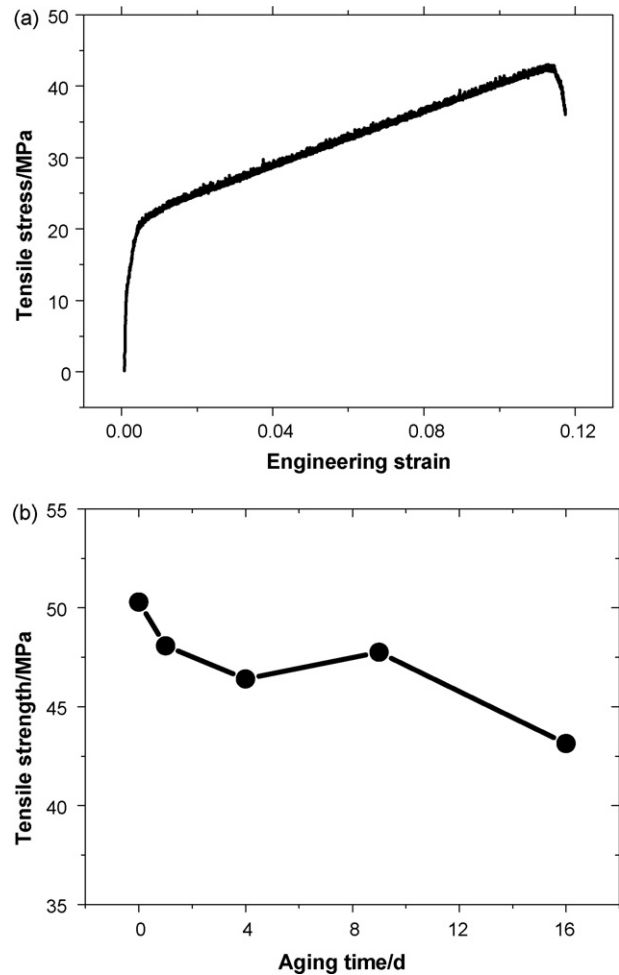

Fig. 7. (a) The tensile–strain curve of the SAC/Ag single crystal joint aged at 170 °C for 1 day and (b) dependence of the tension strength on the aging time for SAC/Ag single crystal joint at 170 °C.
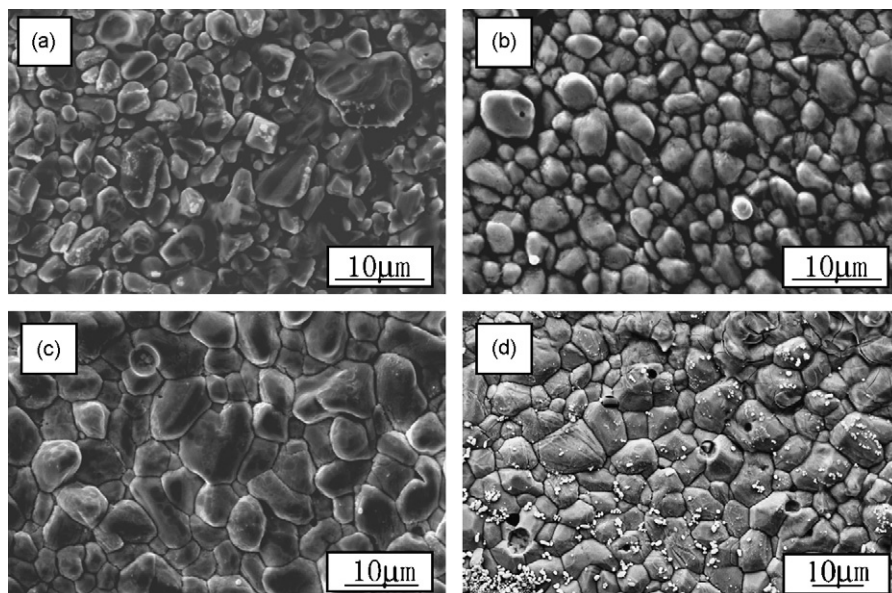

Fig. 8. Morphologies of IMCs exposed by erosion: (a) as-reflowed, aged at 170 °C for (b) 1 day, (c) 4 days and (d) 9 days.
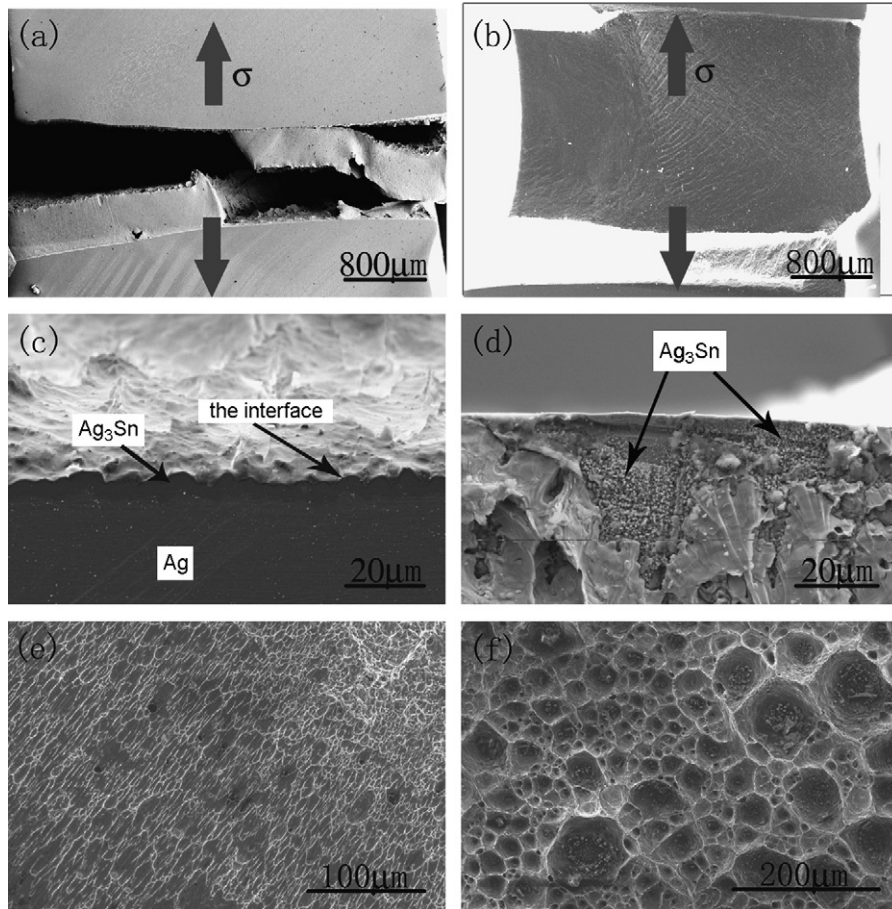
Fig. 9. Tensile fracture morphologies of SAC/Ag single crystal joint: (a) cross-section of step fracture, (b) cross-section of fracture, (c) the cross-section view of the fracture, (d) the top view of fracture surface, (e) the dimple of the aging for 1 day and (f) the dimple of the aging for 9 days.

duce crack in the IMCs. After aging for 16 days, the thickness of the IMCs in Sn–Ag–Cu/Cu joint approximately increases to 10 μm, while the thickness of the current IMCs is less than 6 μm when the Sn–Ag–Cu/Ag joint was aged for 13 days. Therefore, the Sn–Ag–Cu/Ag joint interface has a better mechanical property than the Sn–Ag–Cu/Cu joint interface after aging due to a relatively low growth speed of the IMCs.

Fig. 8 demonstrates the dependence of the average grain size of the Ag_3Sn IMCs on the aging time. The grains of the as-reflow sample are very loose while the grains of the aged samples are more closely. With increasing aging time, the grains of IMCs grow gradually and become more and more closely. As a result, the roughness of the IMCs or the contact area between the solder and the IMCs decreases, which might be one of the reasons why the tensile strength of the Ag/SAC joints gradually drop, as shown in Fig. 7(b).

Fig. 9 shows the macroscopic and microscopic tensile deformation and fracture morphologies of the Ag/SAC joints aging for different days. Normally, there are two kinds of fracture modes in the joint samples, i.e. step fracture and flat fracture [36], as shown in Fig. 9(a) and (b). But in this study, it seems that there is no a clear transition in the fracture mode from step fracture to flat fracture with increasing aging time. Fig. 9(c) and (d) are the cross-section and the top view of the fracture interface, the

fracture basically occurred along the Ag_3Sn/SAC solder interface at the edge of the joint sample. From Fig. 9(d), it can be seen that on the Ag substrate side there are many IMC particles at the edge of the sample, which were identified as Ag_3Sn phase by EDX. It indicates that the joint strength of SAC/Ag is strong enough and the plastic strain near the interface is high for the SAC solder. Fig. 9(e) and (f) shows the fracture surfaces of the joint samples aging for 1 and 9 days and there are some differences in fracture modes in details. For samples aging for short time, there is no or less IMC particles within the dimples, which displays clear ductile feature (see Fig. 9(e)), indicating that the fracture mainly occurred in a shear mode within the SAC solder. For samples aging for long time, there exist many IMC particles nearly within every dimple, as shown in Fig. 9(f), and the shear fracture mainly occurred in a combination mode within both the SAC solder and the brittle IMC particles. The reason is that there are many sources of dimples formed between the solder and IMCs for some local brittle particles near the SAC/IMC interface due to the growth of the IMC layer after aging for a long time.

Based on the experimental observations above, the tensile facture processes of the SAC/Ag joint samples can be illustrated as in Fig. 10. Firstly, the soft solder initially accommodated a high local plastic strain, displaying a local necking near the sol-
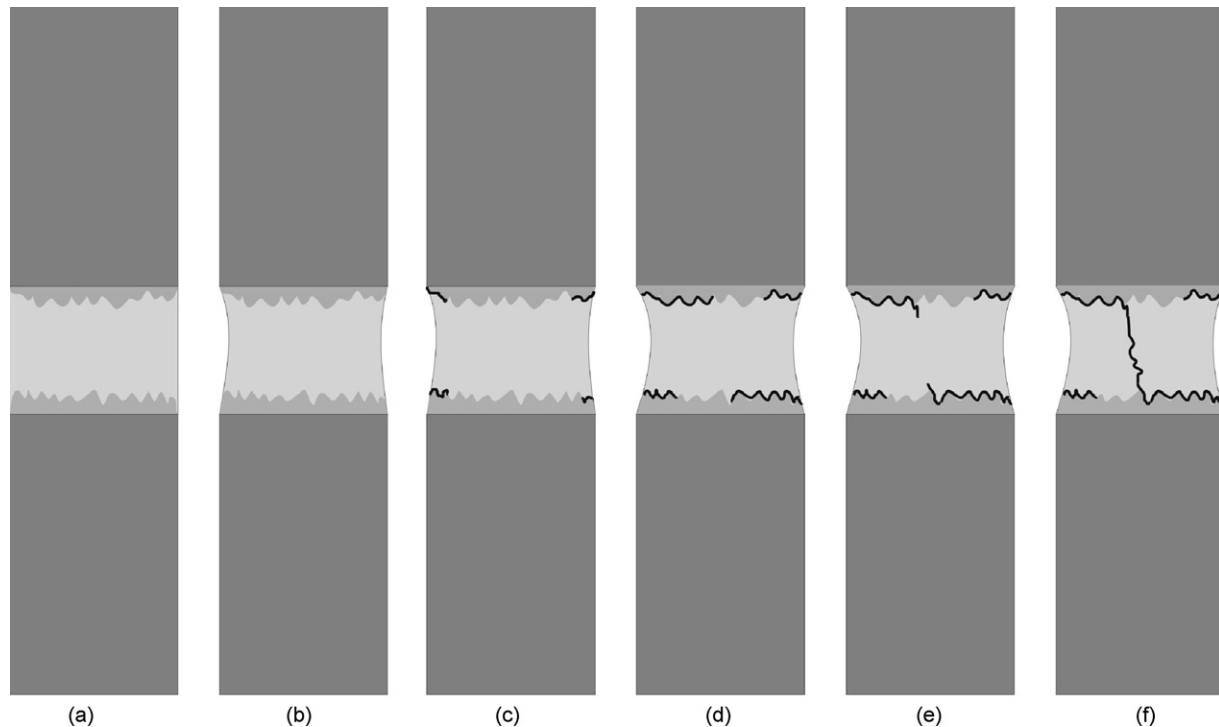
Fig. 10. Illustration of the damage fracture processes at the interface of SAC/Ag single crystal joint under the tensile stress: (a) load tensile stress, (b) elastic strain in the solder, (c) crack nucleated at the edge of the sample, (d) crack grow along the SAC solder/Ag interface, (e) the perpendicular crack nuclear and (f) fracture in the solder.

der/IMC interface (see Fig. 10(b)). Then there was a local shear stress at the edge of the SAC solder/IMC interface, which is easy to induce a small crack along the SAC solder/IMC interface of the sample edge, as in Fig. 10(c). After that, the small crack continued to propagate along the interface of solder/IMC under the external tensile stress due to the plastic strain incompatibility near the interface, as illustrated in Fig. 10(d). When the two interfacial cracks from two different directions propagated certain distance away from the sample edge (see Fig. 10(e)), the high shear stress easily connected the two cracks, forming the final shear fracture through the solder, as illustrated in Fig. 10(f). On the other hand, it can be seen that there are less IMC particles in the dimples for the samples aging for short time and many IMC particles in most dimples for the samples aging for long time (Fig. 9(e) and (f)). The less IMC particles in the dimples should be due to a relatively thin IMC layer, indicating a ductile fracture feature of solder/IMC layer. However, the thick IMC layer will make the interface brittle, bring residual stress and cause many sources of the dimples, leaving many IMC particles in most dimples and leading to a slight decrease in the fracture strength when the SAC/Ag joint samples were aged for a long time.

4. Conclusions

Based on the experimental results and analysis above, the following conclusions can be drawn:

(1) Microstructure evolution of the IMCs between the Sn–Ag–Cu solder and silver single crystal substrate was observed during the solid-state aging. It is found that the IMC phase only consists of Ag_3Sn, however, Ag_5Sn phase was not observed in all the joint samples. During the solid-state aging, the scallop-like Ag_3Sn IMC layer was gradually transformed into planar layer. The growth kinetics of Ag_3Sn IMC shows a diffusion-control mechanism and the diffusion coefficient D was calculated to be about $2.50 \times 10^{-17} \, m^2 \, s^{-1}$ for the solid-state aging. The grain size of the IMCs grew with increasing aging time.

(2) When Sn–Ag–Cu/Ag joint interface is under the liquid-state aging, with increasing aging time, the morphology of IMCs was not transformed into the planar type, but shows a higher roughness. It was also observed that there was only Ag_3Sn phase between Ag/Sn–Ag–Cu solder interface. The thickness of Ag_3Sn IMCs had a linear relationship with the square root of aging time, indicating that the growth kinetics of the Ag_3Sn layer is also diffusion-control and the diffusion coefficient D was measured to be about $1.60 \times 10^{-14} \, m^2 \, s^{-1}$.

(3) The tensile strength of the SAC/Ag joint slightly decreased with increasing aging time, indicating that aging did not cause a serious deterioration for the Sn–Ag–Cu/Ag interface. The tensile strength of the Ag/Ag_3Sn interface is higher than that of the SAC/Ag_3Sn interface. The tensile cracking firstly occurred along the SAC solder/Ag_3Sn interface at the brim of samples due to the local shear stress. Then the crack propagated along the SAC solder/Ag_3Sn interface under the external tensile stress due to the plastic strain incompatibility near the interface. Finally, the cracks from the different directions will merge to a long shear crack through the solder.

Acknowledgements

References

[1] M. Abtew, G. Selvaduray, Mater. Sci. Eng. R 27 (5–6) (2000) 95.
[2] M.J. Rizvi, Y.C. Chan, C. Bailey, H. Lu, M.N. Islam, J. Alloys Compd. 407 (2006) 208.
[3] X. Hong, W.H. Conrad, Metall. Mater. Trans. A 26 (1995) 459.
[4] G. Ghosh, Acta Mater. 48 (14) (2000) 3719.
[5] X. Chen, Int. J. Fatigue. 28 (2006) 757.
[6] M. He, Z. Chen, G.J. Qi, Acta Mater. 52 (2004) 2047.
[7] A. Sharif, Y.C. Chan, Mater. Sci. Eng. B 106 (2004) 126.
[8] C. Kanchanomai, Y. Mutoh, Scripta Mater. 50 (2004) 83.
[9] Y.-H. Lee, H.-T. Lee, Mater. Sci. Eng. A 444 (2007) 75.
[10] J. Shen, Y.C. Liu, Y.J. Han, Y.M. Tian, H.X. Gao, Mater. Sci. Eng. A 441 (2006) 135.
[11] J.-W. Yoon, S.-B. Jung, J. Alloy Compd. 359 (2003) 202.
[12] J.-W. Yoon, S.-B. Jung, J. Alloy Compd. 396 (2005) 122.
[13] T. Ichitsubo, E. Matsubara, K. Fujiwara, M. Yamaguchi, H. Irie, S. Kumamoto, T. Anada, J. Alloy Compd. 392 (2005) 200.
[14] J.-W. Yoon, S.-W. Kim, S.-B. Jung, J. Alloy Compd. 391 (2005) 82.
[15] F.J. Wang, X. Ma, Y.Y. Qian, Scripta Mater. 53 (2005) 699.
[16] Y.-S. Kim, K.-S. Kim, C.-W. Hwang, K. Suganuma, J. Alloy Compd. 352 (2003) 237.
[17] M. Date, T. Shoji, M. Fujiyoshi, K. Sato, K.N. Tu, Scripta Mater. 51 (2004) 641.
[18] L.T. Chen, C.M. Chen, J. Mater. Res. 21 (4) (2006) 962.
[19] M.G. Cho, P.W. Paik, H.M. Lee, S.W. Booh, T.G. Kim, J. Electron. Mater. 35 (1) (2006) 35.
[20] Y.T. Huang, T.H. Chuang, Z. Metallkd. 12 (2000) 1002.
[21] B.Y. Wu, H.W. Zhong, Y.C. Chan, M.O. Alam, J. Mater. Res. 21 (9) (2006) 2224.
[22] M.N. Islam, Y.C. Chan, A. Sharif, M.J. Rizvi, J. Alloy Compd. 396 (2005) 217.
[23] M.D. Cheng, S.S. Wang, T.H. Chuang, J. Electron. Mater. 31 (3) (2002) 171.
[24] Y.-W. Yen, C.-C. Jao, C. Lee, J. Mater. Res. 21 (12) (2006) 2986.
[25] K.S. Kim, S.H. Huh, K. Suganum, J. Alloy Compd. 352 (2005) 226.
[26] P. Sun, C. Andersson, X.C. Wei, Z.N. Cheng, D.k. Shangguan, J. Liu, J. Alloy Compd. 425 (2006) 191.
[27] D.Q. Yu, J. Zhao, L. Wang, J. Alloy Compd. 376 (2004) 170.
[28] G. Ghosh, J. Electron. Mater. 33 (10) (2004) 1080.
[29] Q.S. Zhu, Z.F. Zhang, J.K. Shang, Z.G. Wang, Mater. Sci. Eng. A 435–436 (2006) 588.
[30] Y.H. Xia, X.M. Xie, C.H. Lu, J.L. Chang, J. Alloy Compd. 417 (2006) 143.
[31] H.L.J. Pang, K.H. Tan, X.Q. Shi, Z.P. Wang, Mater. Sci. Eng. A 307 (2001) 42.
[32] K. Yamanaka, Y. Tsukada, K. Suganuma, Scripta Mater. 55 (2006) 867.
[33] S. Ishikawa, E. ashino, T. Kono, K. Tatsumi, Mater. Trans. 46 (11) (2005) 2351.
[34] D.Q. Yu, C.M.L. Wu, C.M.T. Law, L. Wang, J.K.L. Lai, J. Alloy Compd. 392 (2005) 192.
[35] J. Gorlich, G. Schimitz, K.N. Tu, Appl. Phys. Lett. 86 (5) (2005) 53106.
[36] G.Y. Li, B.L. Chen, X.Q. Shi, C. Stephen, K. Wong, Z.F. Wang, Thin Solid Films 504 (2006) 421.
[37] H.-T. Lee, M.-H. Chen, H.-M. Jao, T.-L. Liao, Mater. Sci. Eng. A 358 (2003) 134.